GEOPHYSICAL RESEARCH LETTERS, VOL. 25, NO. 5, PAGES 675-678, MARCH 1, 1998

Evidence for an anisotropic lower mantle beneath eastern Asia: Comparison of shear-wave splitting data of SKS and P660s

Takashi Iidaka & Fenglin Niu

Earthquake Research Institute, the University of Tokyo

Abstract. Anisotropy in the lower mantle is studied by measuring the difference of the splitting parameter τ (the delay time between two split shear-waves) between the two phases SKS and P660s. These two phases are the P-to-S conversion waves at the CMB and the 660-km discontinuity, and therefore are affected by the accumulated anisotropy of whole and upper mantle, respectively. An approximately 0.4 sec time difference of τ value between SKS and P660s is observed at the station HIA, a CDSN broadband seismic station located in central China. This difference is supposed to be caused by the accumulated anisotropy in the lower mantle beneath the eastern Asia region. If the anisotropy is assumed to be distributed uniformly in the whole lower mantle or a lowermost 300-km D" layer, the resulted anisotropy will be 0.08% and 0.5%, respectively. However, the real intensity of the existing anisotropy in the studied region may be much larger than the above values, depending on its size and location in the lower mantle.

Introduction

Study of the elastic anisotropy in the lower mantle is important to reveal the mantle dynamics. An elastic anisotropy is seismologically studied by using waveform splitting, which is often observed in the shear waves arrivals. The splitting parameter τ, which is the delayed time between the fast and slow components of a shear wave, is defined to quantify waveform splitting. Most of the recent works on the mantle anisotropy used the teleseismic wave SKS [e.g. *Silver and Chan*, 1991]. Due to its P-to-S conversion at the core-mantle boundary (CMB) of the receiver side, the waveform of SKS is splitted only by the mantle anisotropy in the receiver side. Global investigations [e.g. *Silver and Chan*, 1991, *Vinnik et al.*, 1992] suggest that the mean value of τ for SKS is about 1 sec. The observed 1 sec splitting of SKS waveform is the accumulated effect of the whole mantle anisotropy. However, it is usually interpreted to be caused by the upper mantle anisotropy, which is associated with tectonic processes. Efforts to constrain the anisotropic region related to the SKS splitting using seismological methods have been made by many researchers. By comparing the waveform splitting data of S, ScS and SKS phases of deep events, *Meade et al.* [1995] concluded that the lower mantle is seismically isotropic, because even though SKS and ScS make one-way and two-way traverses through the lower mantle along near vertical paths, respectively, the observed τ of ScS and SKS are almost same. However, as pointed by *Hiramatsu et al.* [1997], source side anisotropy within a slab is strongly heterogeneous, therefore comparison of ScS with SKS can not be used exactly to infer the anisotropy in the lower mantle. On the other hand, *Marson and Savage* [1997] observed a large discrepancy of τ between SKS and ScS, and suggested a frequency-dependent anisotropy in the Wellington region. *Vinnik and Montagner* [1996] used stacked P-to-S converted waves at the mantle transition zone discontinuities to determine possible anisotropy existing in the mantle transition zone.

In this study, we introduce a comparison of shear-wave splitting between the two phases SKS and P660s, which, as explained in the following text, will allow us to examine the lower mantle anisotropy, if present, more effectively. As shown in the inset of Fig. 1, P660s is a phase that travels most path as a P-wave, and converts to an S-wave at the '660-km' discontinuity just beneath a receiver [*Niu and Kawakatsu*, 1996]. For a receiver with an epicentral distance of approximately 80°, the observed P660s and SKS travel almost the same ray path as an S-wave in the receiver-side upper mantle, but a different way in the lower mantle as a P- and an S-wave, respectively. Therefore, the difference of the

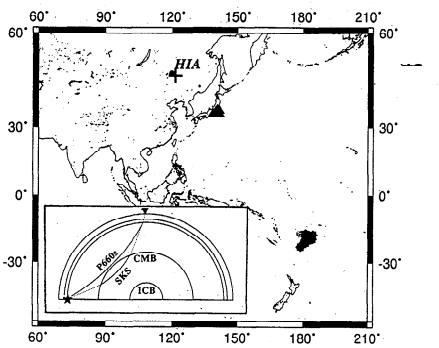

Figure 1. The location map of the earthquakes (stars) and HIA seismic station (circle). The ray paths of the P660s and SKS waves are shown in the inset. The conversion points of the P660s waves at the 660 km discontinuity and SKS at the core-mantle boundary are shown by crosses and triangles, respectively.

Paper number 98GL00297.
0094-8534/98/98GL-00297$05.00

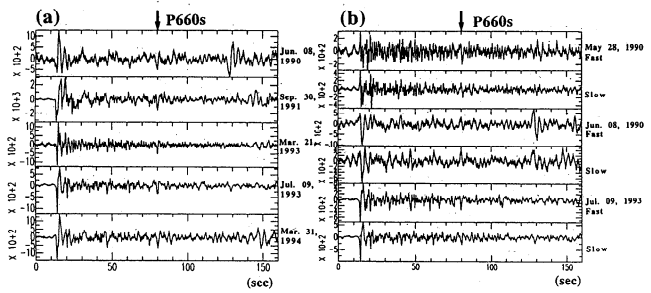

Figure 2. (a) Examples of the wave form of P660s waves. (b) The seismograms of the polarized wave on the fast and slow components are shown.

waveform splitting between SKS and P660s, if observed, can be attributed directly to the anisotropy in the lower mantle where only SKS travels as an S-wave.

Since it is a secondary wave with very small amplitude, P660s is difficult to identify from an individual seismogram, which usually prevents it to be used as a phase to analyze waveform splitting. In this study, in order to get a better S/N ratio we use only the seismograms of deep events. As a result we find a clear P660s phase on many of individual seismograms (Fig. 2) at station HIA (Hailar, China).

Data

As we try to identify the weak signal of P660s, we must ensure that there are no primary phases arriving in the same time window of seismograms. The primary phases such as PP and PcP are candidates for the mask of P660s wave. For this reason, we choose teleseismic events with an epicentral distance of $60 - 90°$. To avoid further interference with pP and sP, we limited hypocentral depths to be deeper than 400 km for the P660s wave.

The ongoing expansion of broadband seismometers all over the world have accumulated a great amount of high quality data. Waveforms of more than one hundred broadband stations are available to us at the present time. We use the broadband data from IRIS Data Management Center. The coverage period is from January 1990 to December 1994. After examining thousands of seismograms, we found out that the HIA station is the only station which we can detect clear isolated P660s wave from most of individual seismograms for the deep events that occurred in the Tonga subduction zone. Geographic distribution of the station HIA and Tonga deep events are shown in Fig. 1. In Table 1, we list the 17 earthquakes used in this study, among which 3 intermediate-depth events are also included. For the records of some deep events, we can not read SKS wave due to its limited length of storage. We therefore included the intermediate-depth events for more SKS data.

Table 1. Earthquakes Used and Parameters Estimated

Date	Time	Lat.	Lon.	Dep.	Mag.	ϕ_{SKS}	τ_{SKS}	ACR-SKS	ϕ_{P660s}	τ_{P660s}	ACR-P660s	Back Az.
(y m dy)	*(h min s)*			*km*	*Mw*	*deg.*	*sec.*	*deg.*	*deg.*	*sec.*	*deg.*	*deg.*
1990 02 02	18 34 46.7	-17.94	-178.38	576.0	5.8	-	-	-	16	0.45	137	122.7
1990 05 20	07 32 36.9	-18.09	-175.34	232.0	6.3	1	0.65	140	*	*	*	120.5
1990 05 28	11 28 48.9	-20.76	-178.08	497.0	5.9	7	0.55	143	9	0.35	147	124.1
1990 06 08	15 05 10.2	-18.70	-178.90	499.0	6.5	-	-	-	92	0.15	130	123.6
1990 08 28	03 16 52.7	-19.43	-175.83	243.0	5.6	9	0.55	140	*	*	*	121.6
1990 10 10	05 54 58.0	-23.35	178.87	594.0	6.1	3	0.50	139	†	†	†	127.9
1991 06 09	07 45 06.6	-20.18	-176.31	305.0	7.0	-9	0.65	125	†	†	†	122.4
1991 06 11	14 32 48.0	-18.13	-178.43	628.0	5.6	6	0.55	144	†	†	†	122.9
1991 06 13	17 18 45.9	-19.93	-175.74	216.0	5.9	-2	0.60	134	*	*	*	121.9
1991 09 30	00 21 47.5	-20.97	-178.61	580.0	7.0	14	0.60	143	-11	0.20	121	124.7
1993 03 21	05 04 59.0	-17.97	-178.53	584.0	6.3	-	-	-	2	0.15	135	122.9
1993 04 20	16 26 19.9	-20.76	-178.72	592.0	5.8	-	-	-	35	0.25	151	124.6
1993 07 09	15 37 55.1	-19.79	-177.54	412.0	6.1	-	-	-	-2	0.05	125	123.2
1993 12 24	05 18 35.1	-21.71	-178.78	445.0	5.8	-	-	-	-3	0.05	135	125.2
1994 03 09	23 28 07.7	-17.77	-178.50	564.0	7.6	-9	0.65	128	87	0.10	131	122.8
1994 03 31	22 40 53.4	-21.95	-179.58	591.0	6.5	-	-	-	9	0.30	143	125.9
1994 04 20	23 35 30.1	-17.78	-178.45	542.0	5.9	-	-	-	28	0.05	155	122.7

-: (SKS) Not observed due to the limited length of records; *: (P660s) Not detected for an intermediate-depth event; †:(P660s) Not observed due to the limitedS/N ratio. *ACR*: Anisotropy Corrected Azimuth.

Analysis

In the shear-wave splitting analyses, seismic rays with small incident angles should be used to avoid possible distortions in waveform. In order to isolate the lower mantle anisotropy we must compare two waves which have almost similar ray path above the '660-km' discontinuity. From the inset of Fig. 1, we found SKS and P660s waves are suitable phases for this purpose.

We investigate the shear-wave splitting using the techniques employed by *Fukao* [1984]. After the seismic signals of SKS and P660s are picked up from individual seismograms, the following process is then used to determine the shear-wave splitting. The observed SKS and P660s waves are first divided into two orthogonal components. The two waveforms on the two orthogonal components are then rotated with a spacing of 1 degree azimuthal intervals. Finally the cross-correlation coefficient is calculated with one sample of time intervals at each 1 degree azimuthal intervals. The time lag τ (in seconds) and the fast polarization azimuth ϕ (in degree) which yield the maximum correlation are taken to be the best measurements of the delay and axis of symme-

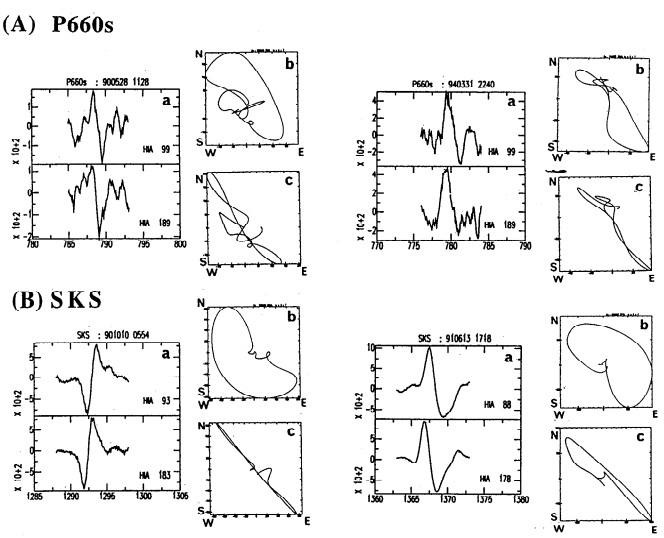

Figure 3. The rotated wave forms(a) with maximum correlation of the (A) P660s and (B) SKS waves. The particle motion diagrams of the observed (b) and anisotropy corrected(c) waves are also shown.

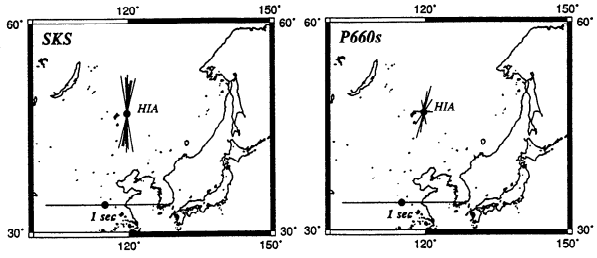

Figure 4. Polarized azimuths of maximum-velocity phase and time delay between maximum and minimum velocity phases of P660s (right figure) and SKS (left figure) waves are shown by the direction and length of the bar, respectively.

try (fast axis) of the anisotropic medium, respectively (Fig. 3). The obtained values of rotation azimuth and time lag are checked as follows. Anisotropy-corrected seismograms are obtained by a clockwise rotation ϕ and a relative time shift τ. Appropriate rotation and time shift would show a linear orbit, which is expected to be the radial direction, in the resultant particle motion diagram. The data indicating linear orbits obtained from anisotropy-corrected seismograms are used to exclude artificial results in which waveforms were distorted by noise.

Results and Discussion

The stable shear-wave splitting data are obtained for SKS waves (Fig. 4, Table 1). The SKS waves are polarized about north-south direction with the τ values of about 0.6 sec (Fig. 4, Table 1). On the other hand, splitting data of τ and ϕ from P660s waves are scattered. Most of the data are polarized to the north-south direction. The time lag data are obtained to be around 0.2 sec.

If the radial directions from the earthquakes to the station are almost parallel or right-angled to the polarization direction of the mantle, the observed data will not be split even if large anisotropic area is located. As the radial directions of the earthquakes with very small τ values of P660s waves are neither parallel nor right angled to the polarization direction, the observed very small polarization data are reliable (Fig. 4, Table 1). The two polarization azimuth data which have an east-west direction might be artificial results caused by small signal to noise ratio. We calculate the averaged and standard deviation values of the observed data with an azimuthal window from -20° to 40° (Fig. 5). The averaged values of the polarized directions of SKS and P660s waves are obtained to be 9.2° ± 14.9° and 2.2° ± 7.8°, respectively. The time lag values τ are calculated to be 0.59 sec ± 0.05 and 0.21 sec ± 0.14 for SKS and P660s waves, respectively.

If the polarization directions of the anisotropic zone in the upper and lower mantle are different, two anisotropic layers analysis have to be used [e.g., *Silver and Savage*, 1994]. The waveform of SKS wave should be also distorted because the SKS wave travels two different polarized areas. In our results, similar polarization directions were observed for both of the P660s and SKS waves, and simple SKS waveforms were observed. The accumulated lower mantle contribution to τ can be obtained as the time difference between the splitting values of SKS and P660s waves. We conclude that the accumulated lower mantle time delay of shear wave splitting is about 0.4 sec in our study area.

Since SKS travels more than 3000 km in the lower mantle, it is difficult to determine which part of the lower mantle deforms the SKS waveform. If we assume anisotropy is uniformly distributed in the whole lower mantle, then our result indicates that only about 0.08% anisotropy exists in the vast lower mantle. Since there are several studies suggest that no contribution of shear-wave splitting from the lower mantle [e.g., *Meade et al.*, 1995; *Iidaka and Obara*, 1995], it seems that the anisotropy in the lower mantle should be heterogeneous.

The observed 0.08% anisotropy in the lower mantle is small. A range of measurements and theoretical calculations indicate that all possible lower mantle minerals are significantly anisotropic: 11.1% for MgO [*Jackson and Niesler*, 1982], and 16.4% for cubic-structured $MgSiO_3$ perovskite [*Cohen*, 1987]. The following possible interpretations, which were suggested by *Meade et al.* [1995] for isotropic lower mantle model, might be adopted. Those are (1) lower mantle mineral assemblages maintain random textures during deformation and recrystallization, (2) the lower mantle is anisotropic on short length scale, but it appears isotropic when the signal is averaged over long ray paths, (3) the magnitude of strain in the lower mantle is not adequate for texture development, or (4) the intrinsic elastic anisotropy values described above are sensitive to pressure and temperature, it is unlikely that any of these minerals will become elastically less anisotropic under lower mantle conditions.

The D" layer lies at the bottom of the earth's rocky mantle, and separates it from the liquid metal-alloy core. *Lay and Helmberger* [1983] presented the first definitive evidence for a D" discontinuity 250-300 km

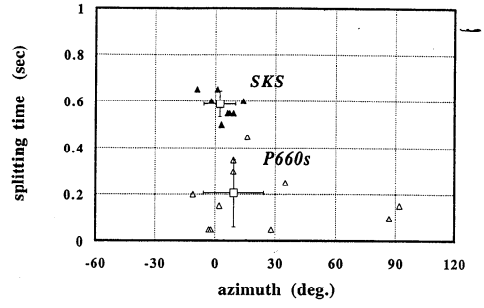

Figure 5. Polarized azimuth data of maximum-velocity phase and time delay data of P660s and SKS waves are plotted by open and closed triangles, respectively. Polarized azimuth is indicated by the clockwise rotation azimuth from north (0°). The averaged and standard deviation values, which were calculated with the azimuthal window from -20° to 40°, are shown by squares and bars, respectively.

above the core-mantle boundary(CMB); later analyses of P- and S-wave data have revealed that the discontinuity exhibits strong lateral variations and is not a global feature [e.g. *Lay and Helmberger*, 1983; *Garnero et al.*, 1993]. Observations of lithospheric seismic anisotropy have provided valuable insight into the nature of the upper mantle boundary layer, but discussion of lower-mantle seismic anisotropy has been somewhat contentious. It has also been proposed that D" layer may be anisotropic [e.g., *Vinnik et al.*, 1989; *Kendall and Silver*, 1996].

Summarizing these previous works, we can see that the D" region is a strong heterogeneous layer with large transverse anisotropy. However, a few previous studies suggest that possible azimuthal anisotropy exists in this layer [*Marson*, 1997]. Therefore, if most of the lower mantle is isotropic and the observed 0.4 sec difference of τ is caused by the lowermost D" layer, then our result will suggest the D" region is also an azimuthal anisotropic layer. Assuming that the observed anisotropy is distributed uniformly in the D" layer with a thickness of 250 - 300 km, then the averaged anisotropy is estimated to be approximately 0.5 - 0.6% along the path length, which is small compared with the averaged transverse anisotropy values of 1.8% in D" obtained by *Kendall and Silver* [1996].

Conclusion

By comparing the waveform splitting observed in SKS and P660s, we have shown that seismic anisotropy really exists in the lower mantle beneath eastern Asia, although we can not restrict which parts of the lower mantle should be attributed. This result is preliminary in the sense that we have investigated only one seismic station, and a world-wide mapping of the lower mantle anisotropy is inevitable to understand its geophysical implications.

Acknowledgments. We thank Dr. Kaneshima and Prof. Kawakatsu for helpful discussions. SAC (Seismic Analysis Code) was used in our calculation. This research was supported by a grant from Japanese Ministry of Education, Science and Culture.

References

Cohen, R. E., Elasticity and equation of state of $MgSiO_3$ Perovskite, *Geophys. Res. Lett.*, *14*, 1053-1056, 1987.

Fukao, Y., Evidence from core-reflected shear waves anisotropy in the Earth's mantle. *Nature*, *309*, 695-698, 1994.

Garnero, E. J., D. V. Helmberger, and S. Grand, Preliminary evidence for a lower mantle shear wave velocity discontinuity beneath the central Pacific, *Phys. Earth Planet. Int.*, *79*, 335-347, 1993.

Hiramatsu, Y., M. Ando, and Y. Ishikawa, ScS wave splitting of deep earthquakes around Japan, *Geophys. J. Int.*, *128*, 409-424, 1997.

Iidaka, T., and K. Obara, Shear-wave polarization anisotropy in the mantle wedge above the subducting Pacific plate, *Tectonophys.*, *249*, 53-68, 1995.

Jackson, I., and H. Niesler, The elasticity of periclase to 3 GPa and some geophysical implications, in *High Pressure Research in Geophysics*, edited by S. Akimoto and M. H. Manghnani, pp. 93-113, Center for Academic Publications, Tokyo, 1982.

Kendall J. -M., and P. G. Silver, Constraints from seismic anisotropy on the nature of the lowermost mantle, *Nature*, *381*, 409-412, 1996.

Lay T., and D. V. Helmberger, A lower mantle S-wave triplication and the shear velocity structure of D", *Geophys. J. R. astr. Soc.*, *75*, 799-837, 1983.

Marson, K., Seismic anisotropy in the Wellington region: shear-wave splitting results, *Inst. Geophys. Report Victoria Univ.*, 32pp, 1997.

Marson, K., and M. K. Savage, Frequency-dependent anisotropy in the Wellington region, New Zealand, submitted to *Geophys. Res. Lett.*.

Meade, C., P. G. Silver, and S. Kaneshima, Laboratory and seismological observations of lower mantle isotropy, *Geophys. Res. Lett.*, *22*, 1293-1296, 1995.

Niu, F., and H. Kawakatsu, Complex structure of the mantle discontinuities at the tip of the subducting slab beneath the northeast China: a preliminary investigation of broadband receiver functions, *J. Phys. Earth*, *44*, 701-711, 1996.

Silver, P. G., and M. K. Savage, The interpretation of shear-wave splitting parameters in the presence of two anisotropic layers, *Geophys. J. Int.*, *119*, 949-963, 1994,

Silver, P. G., and W. Chan, Shear wave splitting and subcontinental mantle deformation, *J. Geophys. Res.*, *96*, 16429-16454, 1991.

Vinnik, L. P., and J. P. Montagner, Shear wave splitting in the mantle Ps phases, *Geophys. Res. Lett.*, *18*, 2449-2452, 1996.

Vinnik, L. P., L. I. Makeyeva, A. Milev, and Y. Usenko, Global patterns of azimuthal anisotropy and deformation in the continental mantle, *Geophys. J. Int.*, *111*, 433-447, 1992.

Vinnik, L. P., V. Farra, and B. Romanowicz, Observational evidence for diffracted SV in the shadow of the earth's core, *Geophys. Res. Lett.*, *16*, 519-522, 1989.

Takashi Iidaka and Fenglin Niu,
Earthquake Research Institute, the University of Tokyo
1-1-1 Yayoi, Bunkyo-ku, Tokyo 113, Japan.
(e-mail [iidaka,niu]@eri.u-tokyo.ac.jp)

(received August 26, 1997;
revised December 5, 1997;
accepted December 25, 1997.)